Available online at www.sciencedirect.com
ScienceDirect
Journal of the European Ceramic Society 27 (2007) 343–350
www.elsevier.com/locate/jeurceramsoc

Microwave sintering of AlN powder synthesized by a SHS method

Cheng-Yu Hsieh[a], Chun-Nan Lin[a], Shyan-Lung Chung[b,*],
Jiping Cheng[c], Dinesh K. Agrawal[c]

[a] Department of Chemical Engineering, National Cheng Kung University, Tainan, 701 Taiwan, ROC
[b] Department of Chemical and Materials Engineering, National University of Kaohsiung, Kaohsiung, 811 Taiwan, ROC
[c] Materials Research Institute, Pennsylvania State University, University Park, PA 16802, USA

Received 29 October 2005; received in revised form 3 March 2006; accepted 11 March 2006
Available online 3 July 2006

Abstract

Sintering of the AlN powder synthesized by a combustion synthesis method, which was developed recently by the present authors, was studied by using a microwave sintering technique. A single mode microwave cavity was used and an insulation package with a simple configuration was developed. A high sintering temperature (1900 °C or higher) and a stable and uniform heating were readily achieved. A temperature measurement technique using a thermocouple with extrapolation was established to obtain the sintering temperature. A percent theoretical density of 99.5% and a thermal conductivity of 186 W/m K were obtained for a specimen which was sintered at 1900 °C with a soaking time of 30 min and 3 wt.% of Y_2O_3 added. The effects of sintering aid (i.e., Y_2O_3) and sintering temperature on densification, microstructure and thermal conductivity of the sintered specimens were investigated.

Keywords: Microwave processing; Sintering; Thermal conductivity; Nitrides; SHS; AlN

1. Introduction

Aluminum nitride (AlN) has been acknowledged as an important industrial material because of its unique combination of properties such as high thermal conductivity, high electrical resistivity, low thermal expansion coefficient, moderately low dielectric constant, good thermal shock resistance and good corrosion resistance.[1,2] It has been considered for many applications such as substrates for power electronics, an insulating material for RF and microwave packages, an electrostatic chuck dielectric for semiconductor processing equipment, heat sinks of mainframes for super-computers, high thermally conductive composite materials, and hardware for containing or processing molten metals and salts.[3,4]

Currently, aluminum nitride has been produced commercially either by carbothermal reduction and nitridation of alumina powder or by direct nitridation of aluminum powder.[5] Although high purity AlN powders can be produced, both methods suffer from high energy consumption and complicated production processes. We have recently developed a combustion synthesis (SHS) method for the synthesis of aluminum nitride.[6] This method has advantages including low energy consumption, simple processing procedure, high production rate and being capable of mass production. As many other SHS methods, the as-synthesized product from our SHS method requires milling in order to obtain powders with desired particle sizes. If an appropriate and effective apparatus is available for milling, the AlN synthesized by our SHS method may find practical applications.

Many applications of AlN powder require sintering as a manufacturing step. Sintering of AlN has usually been carried out by conventional techniques such as pressureless sintering[7,8] and hot pressing.[9,10] Due to covalent bond nature of AlN, the sintering is usually performed under relatively severe conditions such as a high sintering temperature (e.g., 1800 °C or higher) and a long soaking time[7–10] (e.g., 1 h or longer). To avoid cracking of specimens due to non-uniform heating or cooling, the heating and cooling are both usually controlled at very low rates (e.g., 10 °C/min) during the sintering process.[11] The conventional sintering methods for AlN thus suffer from high energy consumption and long operation time (8–12 h).

Application of microwave for sintering ceramic materials has recently attracted much attention.[12] Advantages of microwave

---

[*] Corresponding author. Tel.: +886 6 2757575x62654; fax: +886 6 2344496.
E-mail address: slchung@mail.ncku.edu.tw (S.-L. Chung).

0955-2219/$ – see front matter © 2006 Elsevier Ltd. All rights reserved.
doi:10.1016/j.jeurceramsoc.2006.03.003

heating and sintering include fast heating rate, energy efficiency, volumetric and uniform heating, enhancement of mass transport during sintering, and superior properties of the sintered products.[13–16] For the sintering of AlN, it has been reported that better sintered specimen properties can be realized by microwave sintering as compared to the conventional sintering techniques.[17] However, due to the nature of microwave heating mechanism, a suitable insulation package is required to obtain a high enough temperature for AlN sintering and the package has been usually constructed in a complex design.[15–22]

The present study is aimed at studying the microwave sintering of the AlN powder synthesized by the combustion synthesis method developed recently by the authors as mentioned previously.[6] A simple insulation package was developed and a high sintering temperature (1900 °C or higher) was readily achieved. The effects of sintering aid (i.e., Y_2O_3) and sintering temperature on densification, microstructure and thermal conductivity of the sintered specimens were investigated.

2. Experimental

2.1. Preparation of AlN powder

The AlN powders used in the present study were prepared by our newly developed combustion synthesis method.[6] The as-synthesized AlN product was crushed to under 60 mesh and then milled for 6 h by using an attritor (Union Process, Szegvari Attritor, U.S.A.). AlN balls with 5 mm in diameter and acetone were used as grinding media and milling fluid, respectively. Listed in Table 1 are the properties of the as-synthesized AlN product and the AlN powders thus obtained for microwave sintering in the present study. The oxygen contents were measured with a N/O analyzer (Leco, TC300, U.S.A.). Other impurity concentrations were determined by ICP spectroscopy (Hewlett Packard, 4500, U.S.A.). The particle size distribution was measured by using a centrifugal-sedimentation particle size analyzer (Brookhaven, BI-XDC, U.S.A.).

2.2. Microwave sintering of AlN

In the present study, Y_2O_3 (TG-007, ECHO CHE CO., LTD, 99.99%, D_{50}: 2 μm) was used as sintering aid. The AlN powder, various amounts of the Y_2O_3 (0–7 wt.%) and cellulose (3–5 wt.%, served as binder) were mixed in high purity acetone by using a magnetic stirrer. After mixing, the slurry was dried in a vacuum oven and then was ground. Green compacts with ∼15.5 mm in diameter and ∼5 mm in thickness were obtained by uniaxially pressing the powder at 250 MPa for 2 min and a green density of ∼53% of the theoretical value was obtained.

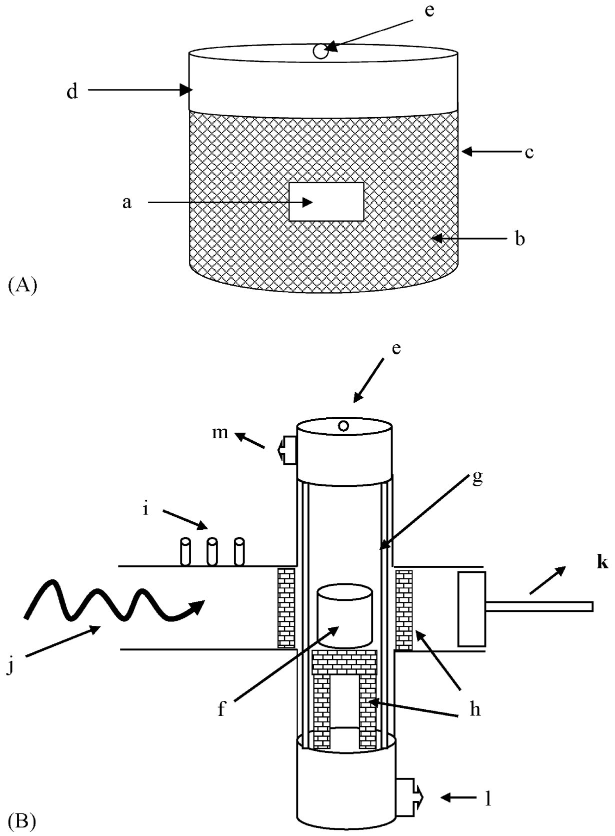

Fig. 1. Schematic illustrations of (A) specimen insulation and (B) microwave cavity: (a) AlN specimen; (b) AlN packing powder; (c) AlN crucible; (d) insulating material; (e) view hole; (f) AlN crucible containing AlN specimen; (g) quartz tube (D_{in}: 46 mm; D_{out}: 50 mm); (h) Al_2O_3 fiber blocks; (i) tuner; (j) microwave source; (k) short adjust; (l) N_2 gas inlet; (m) gas outlet.

The specimen (i.e., the green compact) was placed in an electrical oven to have the binder burned out in air at 350 °C for 0.5 h. The specimen was then placed in an AlN crucible where it was embedded in AlN powder, as shown in Fig. 1(A). The AlN powder (referred to as packing powder) surrounding the specimen was under 60 mesh in size and was highly porous. It was obtained by crushing the as-synthesized AlN product produced by our combustion synthesis method mentioned previously. The AlN crucibles were made by sintering the AlN powder listed in Table 1 with an electrical furnace. Calcium fluoride and yttria were used as sintering aids and the sintering was performed at a sintering temperature of 1600 °C with a soaking time of 3 h. Under such sintering conditions, the AlN crucibles thus obtained were porous and had densities of ∼85% of theoretical. All the crucibles were cylindrical in shape with a thickness of ∼1 mm, a height of 25 mm, and various diameters ranging from 17–40 mm. The packing powder was always made to fill up the crucible and

Table 1
Properties of as-synthesized and ground AlN

AlN	Average particle diameter, D_{50} (μm)	Si (wt.%)	O (wt.%)	Fe (wt.%)	Y (wt.%)
As-synthesized		0.015	0.2	0.012	N[a]
Ground powder	2	0.015	1.5	0.087	0.313

[a] Not detected.

the specimen was placed at the center of the crucible. Effect of the quantity of the packing powder on the sintering could thus be studied by using the crucibles with different diameters.

Fig. 1(B) is a schematic illustration of the microwave cavity. The AlN crucible containing the AlN specimen was placed on a Al_2O_3 fiber support inside a quartz tube (inside diameter: 46 mm), which was installed vertically at the center of the cavity. The quartz tube was surrounded with Al_2O_3 fiber blocks in order to minimize heat loss. The microwave cavity was TE_{103} single-mode and was cooled by circulating water. Microwave at 2.45 GHz was generated by a generator with a power output continuously adjustable in the range of 0–3 KW. The quartz tube was purged with nitrogen at a flow rate of 1 l/min for 10 min before operating. The sintering was performed in a flowing nitrogen gas atmosphere with a flow rate of 450 ml/min. The heating rate was controlled by adjusting the microwave power with a variac. For each sintering experiment, the microwave power was increased by 100 W for every 10 min during heating until reaching the desired sintering temperature and the power was held constant during soaking. After soaking, the microwave power was decreased by 100 W for every 10 min to decrease gradually the specimen's temperature. In the present study, a soaking time of 30 min and a microwave power of either 700 or 400 W were used in all the experiments presented here. The operating time for the sintering process was thus either 150 or 90 min depending on whether a microwave power of 700 or 400 W was used, respectively.

In order to monitor the sintering process, temperature was continuously measured with a two-color pyrometer (Infratherm ISQ5, IMPAC, Germany) which was mounted at a distance above the top of the quartz tube. However, since the radiation received by the two-color pyrometer was mainly emitted by the packing powder covering the specimen, the pyrometer measurement provided the temperature of the packing powder but not the specimen. To gain an idea about the specimen's temperature during sintering (especially during soaking), each sintering experiment was repeated for measurement of specimen's temperature by a thermocouple. To avoid disturbance of the thermocouple to the sintering process, this thermocouple measurement was performed only at the end of the soaking period. Besides, the microwave power was turned off right before the insertion of the thermocouple so that their mutual interference was avoided. In these measurements, the thermocouple (W-type, wire diameter: 0.127 mm) was inserted through the view hole at the top of the quartz tube and then through the packing powder until toughing the specimen.

Two typical temperature–time histories measured by the thermocouple are shown in Fig. 2. Due to heat transfer to the thermocouple from its surrounding, the temperature of each profile increased rapidly as the thermocouple was inserted. It then began to decrease because the microwave power had been turned off and the temperature of the specimen was decreasing. Since the decreasing region of each profile represents the specimen's temperature, the profile in this region is extrapolated to time = 0 (the time at which the microwave power was turned off) to obtain the temperature of the specimen at the end of the soaking period. Since the temperature measured by the two-color pyrometer was found to remain essentially constant during soaking period, the temperature obtained by extrapolating the thermocouple measurement was taken to be the sintering temperature. For example, in the two cases shown in Fig. 2, the sintering temperatures were taken to be 1900 and 1800 °C for which the microwave powers of 700 and 400 W were used, respectively, during soaking. In fact, the sintering experiments presented here were all performed under either of the two sets of conditions as shown in Fig. 2 (except those aimed at studying the effects of packing powders where crucibles of different diameters were used). Since the sintering temperatures and the sintering results were quite reproducible under the same conditions, the sintering temperatures of all the experiments presented here were taken to be either 1900 or 1800 °C depending on whether a microwave power of 700 or 400 W was used, respectively, during soaking.

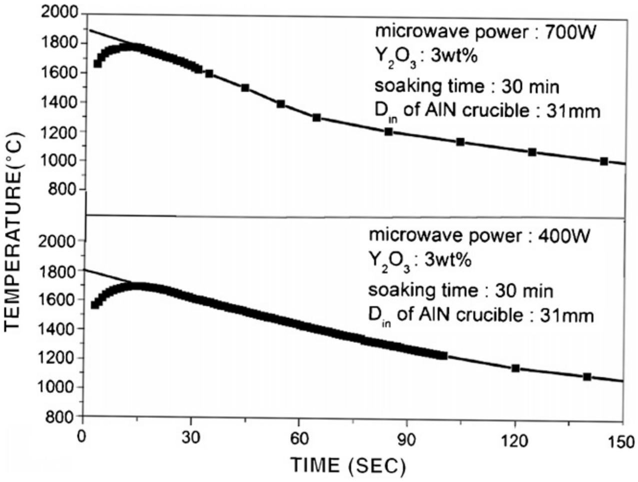

Fig. 2. Typical temperature–time histories measured by a thermocouple after the microwave power was turned off.

The densities of the sintered specimens were measured by Archimedes displacement method using deionized water as the immersion medium. Theoretical densities of the specimens were calculated by assuming that the specimens were composed of AlN and Y_2O_3 according to their percentage contents. The crystalline phases were determined by X-ray diffraction analysis (XRD) (Seifert, XRD7, Germany) and the microstructures were characterized by using a scanning electron microscope (SEM) (Topcon, ABT60, Japan). To measure the oxygen content of the sintered specimens, the sintered specimens were crushed to under 60 mesh and the N/O analyzer mentioned previously was used. The thermal diffusivity was measured by a laser flash method (Holometrix, Microflash 300, U.S.A.). A room temperature heat capacity of 0.718 J/kg K from JANAF thermo-chemical tables was used to calculate the thermal conductivity based on the equation: K (thermal conductivity) = C_p (heat capacity) × ρ(density) × α(thermal diffusivity).

3. Results

3.1. Effect of packing powder

It was found that the quantity of the packing powder affects the maximum temperature that the specimen can achieve when

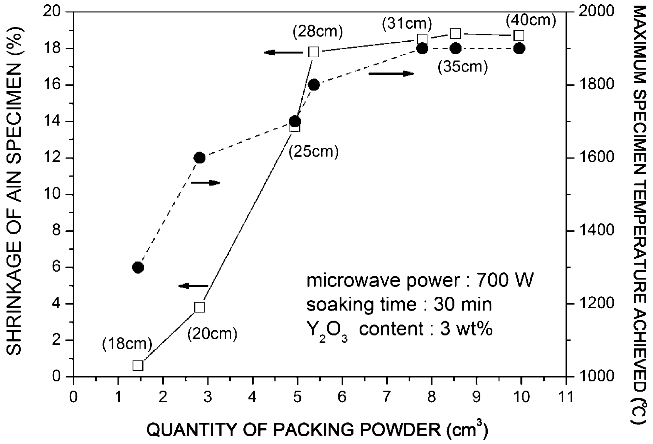

Fig. 3. Effect of the quantity of the packing powder on the maximum temperature achieved and on the shrinkage of the AlN specimen. The inside diameters of the crucibles are indicated beside the data points.

applying the same level of the microwave power. As a result, the shrinkage of the AlN specimen after a certain period of soaking time was also affected by the quantity of the packing powder. Fig. 3 shows these effects under the conditions that the microwave power was 700 W, the soaking time was 30 min, and the Y_2O_3 content was 3 wt.%. As can be seen, both the maximum achievable temperature and the shrinkage of the specimen greatly increase as the quantity of the packing powder increases from 1.5 to 7.8 cm^3. However, they both remain essentially constant as the quantity of the packing powder is increased to beyond 7.8 cm^3. To obtain the highest sintering temperature (and thus the greatest shrinkage), 7.8 cm^3 of the packing powder (i.e., by using a crucible of 31 mm in diameter) was used in all the other sintering experiments presented here.

3.2. Densification of specimen

Under the conditions designed for studying sintering (i.e., those listed in Figs. 4 and 5), the specimens all maintain cylindrical shape and show a uniform shrinkage after sintering. Fig. 4 shows the shrinkage and the density of the specimen as a function of Y_2O_3 content when the sintering temperature is 1900 °C and the soaking time is 30 min (the shrinkages presented in this study were all obtained from measurements of the changes in specimens' diameter). The calculated percent theoretical densities are also presented in the parentheses. As shown in this figure, the density of the sintered specimen increases as the Y_2O_3 content increases from 0 to 7 wt.%. The shrinkage and the percent theoretical density are seen to increase rapidly as the Y_2O_3 content increases from 0 to 3 wt.%, but are relatively unaffected with further increase in Y_2O_3 content. As can be seen, a percent theoretical density of 99.5% or higher can be achieved with a Y_2O_3 content of 3 wt.% or higher at the sintering temperature of 1900 °C.

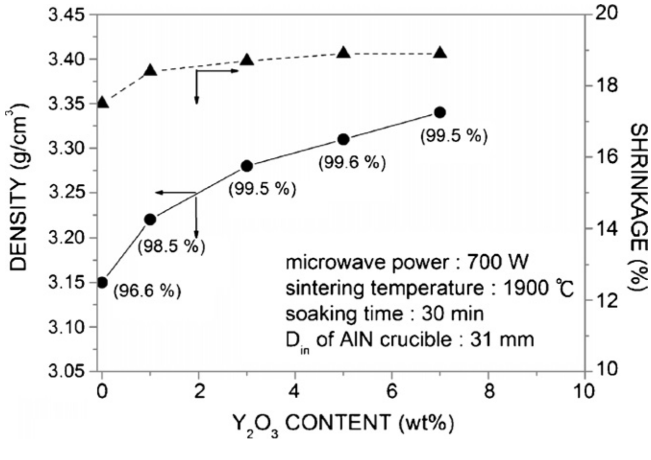

Fig. 4. Effect of the Y_2O_3 content on the shrinkage and the density of the AlN specimen sintered at 1900 °C. The percent theoretical densities are indicated beside the data points.

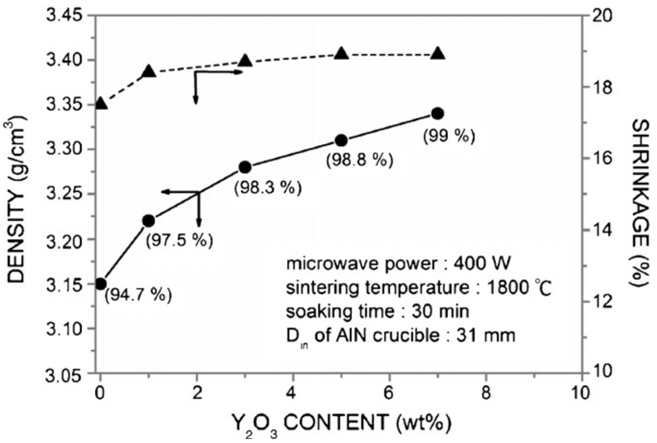

Fig. 5. Effect of the Y_2O_3 content on the shrinkage and density of the AlN specimen sintered at 1800 °C. The percent theoretical densities are indicated beside the data points.

Fig. 5 shows similar measurements to those shown in Fig. 4 but the sintering temperature is 1800 °C. As can be seen, the density, shrinkage and percent theoretical density all have similar trends of variation to those shown in Fig. 4. However, these measured values are all smaller than those obtained at 1900 °C when comparing at the same Y_2O_3 content. The maximum percent theoretical density obtained under such sintering conditions is 99%, which is with 7 wt.% of Y_2O_3 content.

3.3. XRD analysis

At a sintering temperature of 1900 °C, $Al_6O_3N_4$ was the only second phase detected when no Y_2O_3 was added. $YAlO_3$ (YAP) was detected only at 1 and 3 wt.% of Y_2O_3 contents. $Al_2Y_4O_9$ (YAM) was detected at all the Y_2O_3 contents and its intensity (i.e., its quantity) is seen to increase with increasing Y_2O_3 content. Y_2O_3 was detected as the Y_2O_3 content was increased to 5 wt.% or higher. When the specimens were sintered at 1800 °C, the types of second phase were similar to those sintered at 1900 °C with the only difference that $YAlO_3$ (YAP) phase was detected at all the Y_2O_3 contents.

3.4. Thermal conductivity and oxygen content analysis

Shown in Fig. 6 is the effect of the Y_2O_3 content on the thermal conductivity of the specimens sintered at 1900 or 1800 °C.

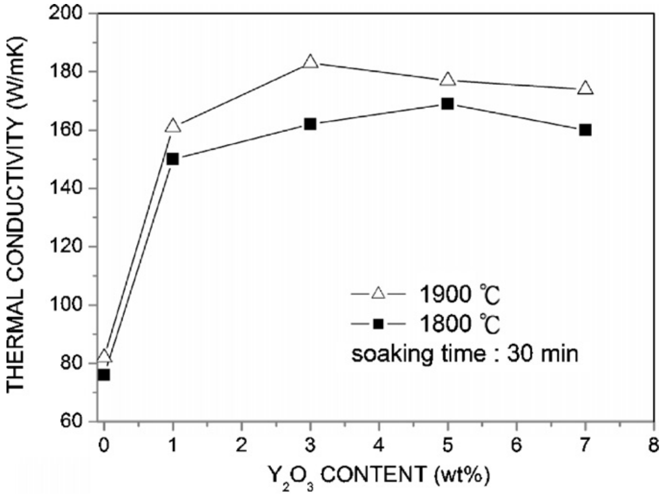

Fig. 6. The thermal conductivities of the specimens sintered at 1900 or 1800 °C with different contents of Y_2O_3.

Without any Y_2O_3 addition, the thermal conductivities are 83 and 77 W/m K when the specimens were sintered at 1900 and 1800 °C, respectively. The thermal conductivity increases significantly with increasing Y_2O_3 content at low content values. For the specimens sintered at 1900 °C, the thermal conductivity reaches its maximum of 186 W/m K at 3 wt.% of the Y_2O_3 content, and it begins to decrease as the Y_2O_3 content is further increased. For the specimens sintered at 1800 °C, the thermal conductivity reaches its maximum of 169 W/m K at 5 wt.% of the Y_2O_3 content and it also begins to decrease with further increase in the Y_2O_3 content. The thermal conductivities obtained at 1900 °C are seen to be higher than those obtained at 1800 °C when comparing at the same Y_2O_3 contents.

The oxygen contents of the specimens with 5 wt.% Y_2O_3 addition were measured after sintering. They were 1.15 and 1.3 wt.% when the specimens were sintered at 1900 and 1800 °C, respectively. Both are noted to be lower than that of the starting powder (i.e., 1.5 wt.%) in spite of the Y_2O_3 addition.

3.5. Microstructure analysis

Shown in Fig. 7 are typical SEM photographs of the fractured surfaces of the specimens sintered at 1900 °C (a and c) or 1800 °C (b and d) with Y_2O_3 contents of 3 or 5 wt.%. At the sintering temperature of 1900 °C, the specimens (Fig. 7(a) and (c)) are seen to be nearly fully dense (with no pores observed). However, the grain and the grain boundary morphology vary with the Y_2O_3 content. With a Y_2O_3 content of 3 wt.% (Fig. 7(a)), the grains are seen to be sharp-edge in shape with a small amount of second phase in the narrow grain boundary. With a Y_2O_3 content of 5 wt.% (Fig. 7(c)), the grain shape is more spherical

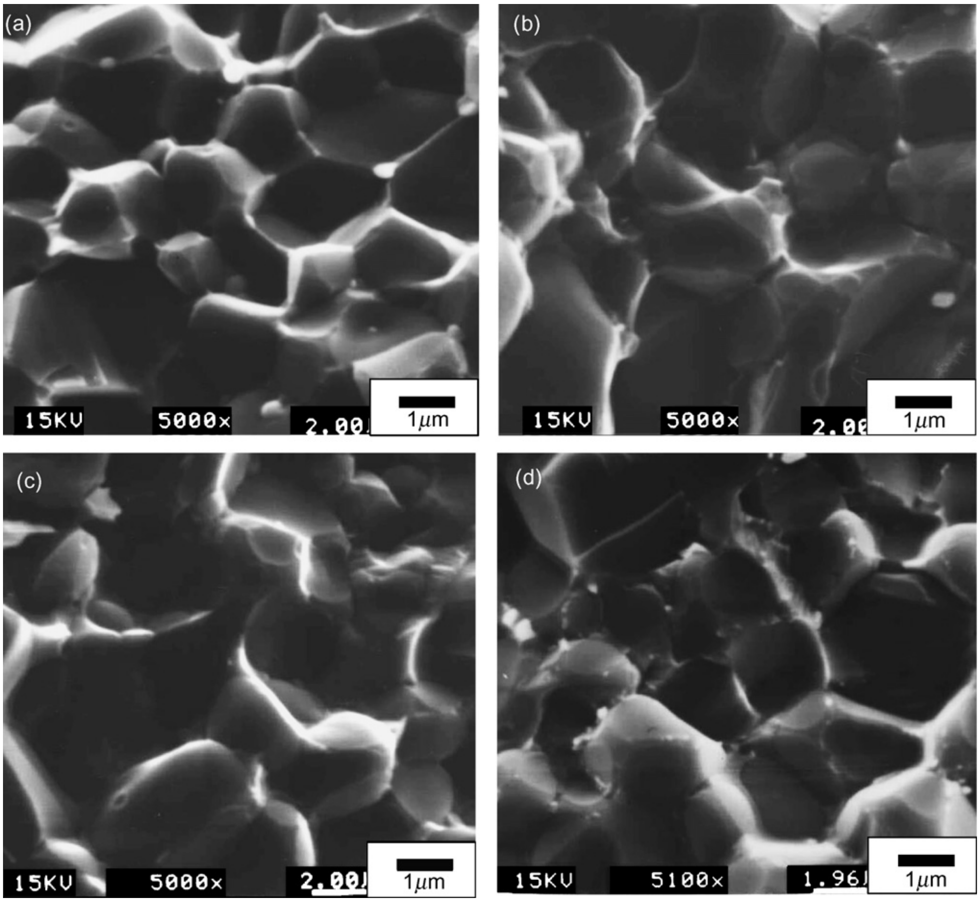

Fig. 7. The typical SEM photographs of the fractured surfaces of the specimens sintered at 1900 °C (a and c) or 1800 °C (b and d) with a Y_2O_3 content of 3 or 5 wt.%, and a soaking time of 30 min.

rather than sharp-edge with a larger amount of second phases along two grain facets. When sintered at 1800 °C, the specimens (Fig. 7(b) and (d)) are observed to have small pores in the second phase region and the grain and grain boundary morphologies are similar to those shown in Fig. 7(c).

Shown in Fig. 8 are SEM photographs of the polished surfaces of the specimens sintered at 1900 °C with a Y_2O_3 content of 3 wt.% (Fig. 8(a) and (b)) or 5 wt.% (Fig. 8(c)). With a Y_2O_3 content of 3 wt.% (Fig. 8(a) and (b)), the distribution of secondary phases (white region) is seen to be more homogeneous and some grains are seen to be contiguous (see Fig. 8(b)). In comparison, more liquid phase pockets and wider grain boundaries are observed with a Y_2O_3 content of 5 wt.% (Fig. 8(c)), which is in accordance with the observation on Fig. 7(c). It is noted that the grain sizes shown in Figs. 7 and 8 are all in the range of 3–6 μm and it seems that the grain size is not related much to the sintering temperature or the amount of sintering aid.

4. Discussion

4.1. Insulation and packing powder

Microwave-sintering process has been found to be significantly influenced by the configuration of the insulation package surrounding the specimens.[15–22] A proper insulation package could reduce heat loss and thus a high sintering temperature could be achieved. It could also avoid arcing and assure a stable and uniform heating. Many researchers[15–22] found that multilayer designs of insulation package were capable of achieving high sintering temperatures. Such multilayer insulation packages are usually composed of several layers of alumina board, porous ceramics and packing powder. They are complicated in configuration and large in volume and thus are not suitable for small cavities. In the present study, a package with a simple configuration was developed and proved to work well that both a high sintering temperature (1900 °C and higher) and a stable and uniform heating were achieved. An insulation material (Al_2O_3 fiber blocks) was used only to surround the quartz tube and to support the AlN crucible (see Fig. 1(B)). The AlN specimen was embedded in AlN packing powder inside the AlN crucible (Fig. 1(A)). The amount of packing powder is seen in Fig. 3 to affect significantly the maximum achievable sintering temperature and thus the shrinkage of the specimen. Although AlN is a thermally conductive material, the packing powder seems to function as an insulator. A high sintering temperature could thus be obtained when an enough volume of the packing powder was used.

Because AlN has a low dielectric loss of 0.0001–0.001 at 1 MHz and room temperature,[23] it is hard to initiate heating with microwave. In many other studies,[15,19–21] a high dielectric loss material such as SiC is usually introduced into the insulation package as a susceptor in the form of powder or rod for sintering of low dielectric loss materials such as AlN, Al_2O_3, ZrO_2 and ZnO. In the present study, no susceptor was used but the specimen could be heated to the desired sintering temperature, i.e., 1900 or 1800 °C, in 60 or 30 min, respectively. These heating times are much shorter than that in conventional heating, which is normally 180–190 min with a frequently used heating rate of ∼10 °C/min.[11] Although AlN does not couple well with microwave at room temperature, it becomes better in absorption of microwave with increasing temperature due

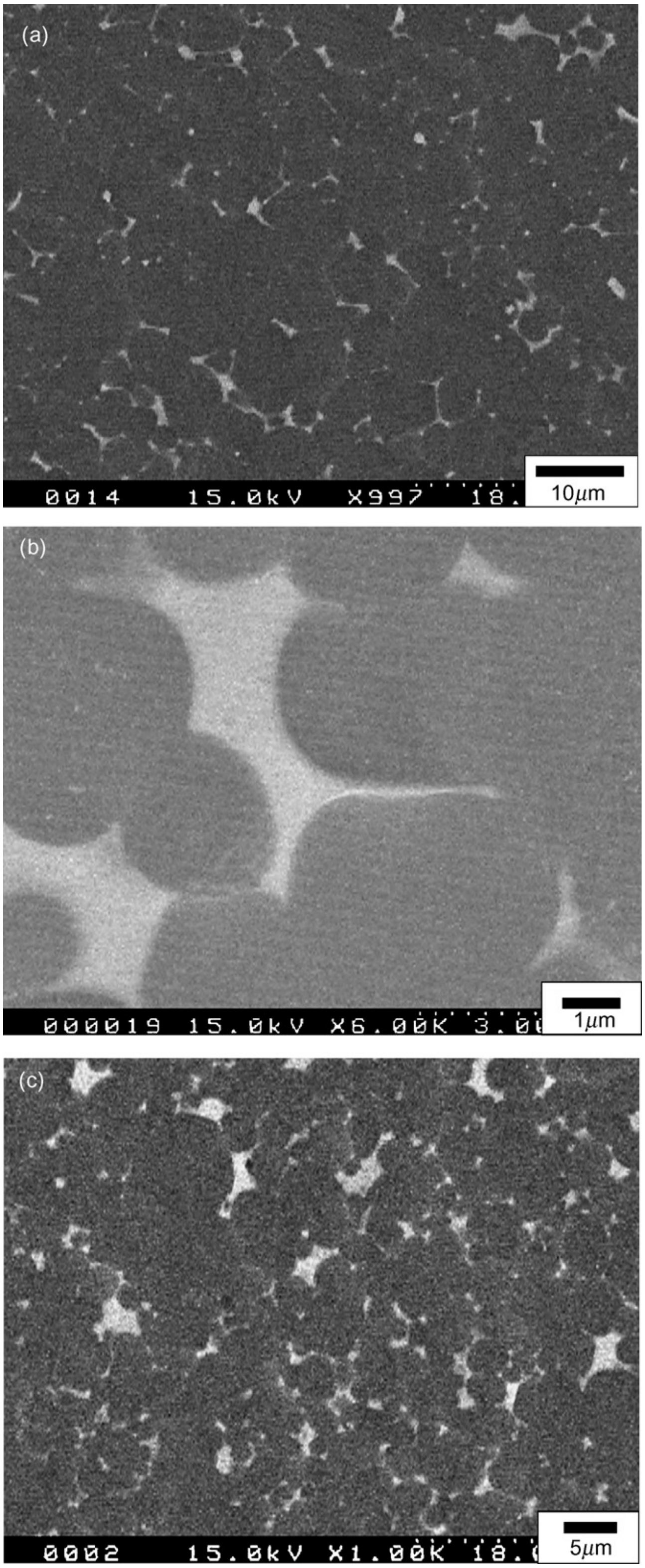

Fig. 8. SEM photographs of the polished surfaces of the specimens sintered at 1900 °C with a Y_2O_3 content of 3 wt.% (a and b) or 5 wt.% (c).

to its increase in dielectric loss. As the temperature of the AlN packing powder increases, the heat loss from the specimen is reduced because the temperature gradient surrounding the specimen is reduced. When an enough volume of the packing powder was used, the packing powder thus functions as a thermal insulator and thus a high sintering temperature can be achieved in a short period of time.

4.2. Thermal conductivity and microstructure

For a multiphase system, the thermal conductivity depends on the thermal conductivities of individual phases, the types and concentrations of impurities, and the microstructure of the specimen. According to the literature,[11] the measured thermal conductivities of the secondary phases encountered in the present study are 7.4 W/m K for YAG, 4.3 W/m K for YAP, 2.5 W/m K for YAM, and 13 W/m K for Y_2O_3 and the theoretical value for AlN is 320 W/m K. For an actual AlN phase, its thermal conductivity may be lower than the theoretical value because of possibly lower degree of densification and impurities involved in the phase. Many previous studies[1,11] have shown that oxygen among various impurities has the most pronounced effect on the thermal conductivity. As shown in Fig. 6, the thermal conductivities are low for the specimens sintered without Y_2O_3 addition (83 and 77 W/m K with sintering temperatures of 1900 and 1800 °C, respectively). Y_2O_3 is considered to exert two effects on the sintering of AlN[24]: (1) to form a liquid phase to enhance densification of the AlN specimen; (2) to act as an oxygen trapper to purify the AlN grain. The thermal conductivities are seen in Fig. 6 to increase significantly as the Y_2O_3 content is increased from 0 to ∼3 wt.%. This is because the densification is enhanced due to the increase in the Y_2O_3 content (see Figs. 4 and 5) and also because the removal of oxygen from inside the grain is enhanced by increasing the Y_2O_3 content.

Although addition of Y_2O_3 can increase the thermal conductivity, higher contents of Y_2O_3 can have an adverse effect because the thermal conductivities of Y_2O_3 and the secondary phases are all much lower than that of the AlN phase. This is seen in Fig. 8 when the Y_2O_3 content is increased to beyond 3 and 5 wt.% for sintering temperatures of 1900 and 1800 °C, respectively. Higher contents of Y_2O_3 are also seen in Figs. 7 and 8 to form thicker secondary phases between the grain boundaries, which act as thermal barriers, thus causing a decrease in thermal conductivity.

The thermal conductivity will be reduced if the high thermal conductivity AlN grain is isolated by the low thermal conductivity secondary phases. As shown in Figs. 7 and 8, the shape of the grains and the distribution of the secondary phases are affected by the sintering temperature and the Y_2O_3 content. When sintered at 1800 or at 1900 °C with a high content of Y_2O_3 (i.e., 5 wt.%), the grains are spherical in shape and are surrounded by secondary phases. When sintered at 1900 °C with 3 wt.% of Y_2O_3 added, the grains are seen to be contiguous and sharp-edge in shape. The contiguous grains are considered to conduct heat better than those surrounded by the secondary phases. Accordingly, the specimen sintered at 1900 °C with 3 wt.% of Y_2O_3 content is measured to have a higher thermal conductivity than others (see Fig. 6).

Sintering temperature also shows an important influence on the thermal conductivity and microstructure. At a higher sintering temperature, the secondary phases wet the grains better due to a lower viscosity and thus a liquid phase sintering proceeds more effectively, resulting in a higher density and a higher thermal conductivity. During sintering, the oxygen can be removed through evaporation or sublimation of secondary phases (e.g., $Al_2O_{(g)}$)[25] and the removal is enhanced with increasing sintering temperature. This is evidenced by the measurement of oxygen content of the sintered specimens. As mentioned previously, the oxygen contents of the sintered specimens were found to be lower than that of the starting powder in spite of the addition of Y_2O_3. Furthermore, the oxygen content of the specimen sintered at 1900 °C was measured to be lower than that of the specimen sintered at 1800 °C. As a consequence, the thermal conductivities obtained at a sintering temperature of 1900 °C are seen to be higher than those obtained at 1800 °C (see Fig. 6). However, due to a relatively short soaking time and possible hindrance of the packing powder to the evaporation of the secondary phases, a certain amount of the secondary phase is still observed along the grain boundaries. A more effective way to remove the secondary phases is thus required to further improve the thermal conductivity of the sintered AlN.

5. Conclusion

Microwave sintering of a combustion synthesized AlN powder has been studied and the thermal conductivity of the specimens sintered under various conditions was measured. A simple insulation package composed of porous AlN powder and an insulation material was developed and proved to work well that both a high sintering temperature and a stable and uniform heating were achieved. A temperature measurement technique using a thermocouple with extrapolation was established to obtain the sintering temperature. A percent theoretical density of 99.5% and a thermal conductivity of 186 W/m K were obtained for a specimen which was sintered at 1900 °C with a soaking time of 30 min and 3 wt.% of Y_2O_3 added. The oxygen content of the sintered specimen was found to be lower than that of starting powder and this was attributed to evaporation of the second phases. A further improvement in thermal conductivity can be expected by applying a more efficient method for removal of the second phases.

Acknowledgement

Support of this research by the National Science Council of the Republic of China under Grant No. NSC 93-2214-E-006-013 is gratefully acknowleged.

References

1. Slack, G. A., Tanzilli, R. A., Pohl, R. O. and Vandersande, J. W., The intrinsic thermal conductivity of AlN. *J. Phys. Chem. Solids*, 1987, **48**, 641–647.

2. Mroz Jr., T. J., Annual materials review: aluminum nitride. *Am. Ceram. Soc. Bull*, 1992, **71**, 782–786.
3. Sheppard, L. M., Aluminum nitride: a versatile but challenging material. *Am. Ceram. Soc. Bull.*, 1990, **69**, 1801–1812.
4. Bachilard, B. and Joubert, P., Aluminum nitride by carbothermal nitridation. *Mater. Sci. Eng. A*, 1989, **109**, 247–251.
5. Selvaduray, G. and Sheet, L., Aluminum nitride: review of synthesis method. *Mater. Sci. Technol.*, 1993, **9**, 463–473.
6. Lin, C. N. and Chung, S. L., Combustion synthesis method for synthesis of aluminum nitride powder using aluminum containers (II). *J. Mater. Res.*, 2004, **19**, 3037–3045.
7. Chen, C. F., Perisse, M. E. and Ramire, A. F., Effect of grain boundary phase on the thermal conductivity of aluminum nitride ceramics. *J. Mater. Sci.*, 1994, **29**, 1595–1600.
8. Pezzotti, G., Nakahira, A. and Tajika, M., Effect of extended annealing cycles on the thermal conductivity of AlN/Y_2O_3 ceramics. *J. Eur. Ceram. Soc.*, 2000, **20**, 1319–1325.
9. Watari, K., Ishizaki, K. and Fujikawa, T., Thermal conduction mechanism of aluminum nitride ceramics. *J. Mater. Sci.*, 1992, **27**, 2627–2630.
10. Hafidi, A., Billy, M. and Lecompte, J. P., Influence of microstructural parameters on thermal diffusivity of aluminum nitride-based ceramics. *J. Mater. Sci.*, 1992, **27**, 3405–3408.
11. Jackson, T. B., Vikar, A. V., More, K. L. and Dinwiddie, R. B., High-thermal-conductivity aluminum nitride ceramics: the effect of thermodynamic, kinetic, and microstructural factors. *J. Am. Ceram. Soc.*, 1997, **80**, 1421–1435.
12. Cheng, J., Agrawal, D., Zhang, Y., Drawl, B. and Roy, R., Fabricating transparent ceramics by microwave sintering. *Am. Ceram. Soc. Bull.*, 2000, **9**, 71–74.
13. Cheng, J., Agrawal, D., Roy, R. and Jayan, P. S., Continuous microwave sintering of alumina abrasive grits. *J. Mater. Proc. Technol.*, 2000, **108**, 26–29.
14. Katz, J. D. and Blake, R. D., Microwave sintering of multiple alumina and composite components. *Am. Ceram. Soc. Bull.*, 1991, **70**, 1304–1308.
15. Ramesh, P. D., Brandon, D. and Schachter, L., Use of partially oxidized SiC particle bed for microwave sintering of low loss ceramics. *Mater. Sci. Eng. A*, 1999, **266**, 211–220.
16. Xu, G. F., Lloyd, I. K., Carmel, Y., Olorunyolemi, T. and Wilson, O. C., Microwave Sintering of ZnO at ultra high heating rates. *J. Mater. Res.*, 2001, **16**, 2850–2858.
17. Xu, G. F., Olorunyolemi, T., Wilson, O. C., Lloyd, I. K. and Carmel, Y., Microwave sintering of high-density, high thermal conductivity AlN. *J. Mater. Res.*, 2002, **17**, 2837–2845.
18. Janney, M. A., Calhoun, C. L. and Kimrey, H. D., Microwave sintering of solid oxide fuel cell materials: I, zirconia-8 mol% yttria. *J. Am. Ceram. Soc.*, 1992, **75**, 341–346.
19. Goldstein, A., Kaplan, W. D. and Singurindi, A., Liquid assisted sintering of SiC powders by MW (2.45 GHz) heating. *J. Eur. Ceram. Soc.*, 2002, **22**, 1891–1896.
20. Xie, Z., Yang, J., Huang, X. and Huang, Y., Microwave processing and properties of ceramics with different dielectric loss. *J. Eur. Ceram. Soc.*, 1999, **19**, 381–387.
21. Brosnan, K. H., Messing, G. L. and Agrawal, D. K., Microwave sintering of alumina at 2.45 GHz. *J. Am. Ceram. Soc.*, 2003, **86**, 1307–1312.
22. Xu, G., Olorunyolemi, T., Carmel, Y., Lloyd, I. K. and Wilson Jr., O. C., Design and construction of insulation configuration for ultra-high-temperature microwave processing of ceramics. *J. Am. Ceram. Soc.*, 2003, **86**, 2082–2086.
23. Data from Ceramic Substrate and Components Ltd.
24. Virkar, A. V., Jackson, T. B. and Cutler, R. A., Thermodynamic and kinetic effects of oxygen removal on the hermal conductivity of aluminum nitride. *J. Am. Ceram. Soc.*, 1989, **72**, 2031–2042.
25. Hundere, A. M. and Einarsrud, M. A., Effects of reduction of the Al–Y–O containing secondary phases during sintering of AlN with YF_3 additions. *J. Eur. Ceram. Soc.*, 1996, **16**, 899–906.